Encyclopedia of Earthquake Engineering
DOI 10.1007/978-3-642-36197-5_51-1

Seismic Tomography of Volcanoes

Ivan Koulakov[a,b]* and Nikolay Shapiro[c]
[a]Trofimuk Institute of Petroleum Geology and Geophysics, SB RAS, Novosibirsk, Russia
[b]Novosibirsk State University, Novosibirsk, Russia
[c]Institut de Physique du Globe de Paris Laboratoire de Sismologie, Paris, France

Synonyms

Ambient noise tomography; Body-wave tomography; Magma sources; Seismic observations on volcanoes; Seismic properties of crust; Seismic tomography

Introduction

Volcano tomography is a branch of geophysics oriented to studying the deep structures beneath volcanoes by means of seismic tomography. **Seismic tomography** is a method for reconstruction of continuous distribution of seismic parameters in 1D, 2D, 3D, or 4D (space and time) using the characteristics of seismic waves traveling between sources and receivers. Seismic parameters to be found in tomographic inversion are in most cases velocities of P and S seismic waves (P and S velocities). For volcanoes, one of the key parameters appears to be the Vp/Vs ratio which can be used to evaluate the content of fluids and melts. Besides the velocity distributions, seismic tomography may provide the information on the anisotropy of seismic parameters which helps studying regional stresses and space-oriented geological structures. In some tomography studies, the target parameter might be the attenuation of P or S waves which may also give important information on magma sources beneath volcanoes.

At all stages of the human history, understanding the mechanisms causing volcano eruptions was one of the most intriguing problems. Until relatively recent time, scientists had only indirect ways to explore processes beneath volcanoes, mainly by making analogies with geological signatures of ancient magmatic systems. During the last decades, the advancement of geophysical methods made possible direct observations of deep structures beneath presently active volcanoes which give precious information about general mechanism of working the volcanic systems. Among all geophysical methods, seismic tomography is one of the most powerful and effective approaches to look at great depths below the volcanoes. Using powerful artificial and natural sources of seismic signal makes it possible getting the information from depths where the main magma sources are located.

Observation Schemes

The configurations and characteristics of observation systems in seismology depend on the properties and sizes of the target objects, as well as on the type of seismic sources. In case of volcano seismology, the parameters of the target volume depend on the type of volcanoes. For example, the subduction-related volcanoes usually have complex multilevel structures of feeding system which may cover the depths down to 100–200 km. In the case of the hot-spot volcanoes, the initial source of magmatism is related to mantle plumes which may propagate throughout the mantle; however, the magma reservoirs and the

*Email: KoulakovIY@ipgg.sbras.ru

DOI 10.1007/978-3-642-36197-5_51-1

related seismicity are fairly shallow in this case (only the first kilometers of depth). When designing an experiment for tomography studies of volcanoes, one should clearly figure out the target properties and define the configuration of the network according to this. In reality, there are many limitations, such as insufficient amount of instruments and difficulties in access to some areas around a volcano that make impossible deploying an ideal network. In the following section, the major components of the observation systems are described, and some recommendations to optimize the designing of the seismic networks are given.

Seismic Sources

Sources used for seismic imaging of volcanoes can be divided in three categories: human-made sources, earthquakes, and ambient seismic noise. Fully controlled artificial sources are expected to provide the highest accuracy of tomographic images. At the same time, their implementation on volcanoes is very sophisticated and expensive. Another shortcoming of artificial sources is that they cannot be produced at depth. In regions with well-distributed volcanic or local tectonic seismicity, earthquakes may give a distribution of sources plausible for high-resolution seismic tomography. However, many volcanoes do not generate sustained seismicity. In this case, the recently developed methods based on correlations of ambient seismic noise become suitable for imaging volcanic edifices.

Human-Made Seismic Sources

Human-made seismic sources include explosions, vibrators, air-gun shots, and weight (or mass) drops and are usually called **active sources**. There are some onshore experiments which use chemical explosions of sufficiently large magnitude to generate seismic signal propagating to the distances of dozens kilometers and depths of a few kilometers. The problem of such explosions is that they are fairly expensive and thus their number is strongly limited. Furthermore, chemical explosions are not ecologically friendly and they are prohibited in most volcanic areas. In most cases, the surveys based on such sources are used for 2D profiling (Fig. 1c).

An alternative method of active-source onshore generation might be using vibrators which are more ecologically safe compared to explosions. However, for the purposes of volcano tomography, the vibrators should be sufficiently powerful and heavy to enable the required propagation of seismic rays. In reality, the transportation of powerful vibrators appears to be not possible in most volcanic areas; therefore, they are not widely used in practice.

In case if a volcano is located close to the seashore, it is possible to use underwater air guns as sources of seismic signal (Fig. 2a). The advantage is that air-gun shots are rather cheap and sufficiently powerful. They can be frequently generated along the ship cruise that gives a huge data base with a clear technology of processing. The problem is that these sources are limited by the shore line and not suitable for most volcanoes.

The major advantage of the active sources is that their parameters are known. The problem is that they are located close to the surface, and seismic signal propagate along the nearly horizontal ray paths. Another problem, which is mostly actual for the air-gun shots, is that they generate very weak S waves which cannot be picked and used for tomography studies.

Earthquakes

Volcanic and tectonic earthquakes located in the volcanic area (including some events located outside the perimeter of the network) are regularly used as sources for seismic tomography of volcanoes (Fig. 1b). The major problem with earthquakes is that their location parameters (coordinates and origin times) are

DOI 10.1007/978-3-642-36197-5_51-1

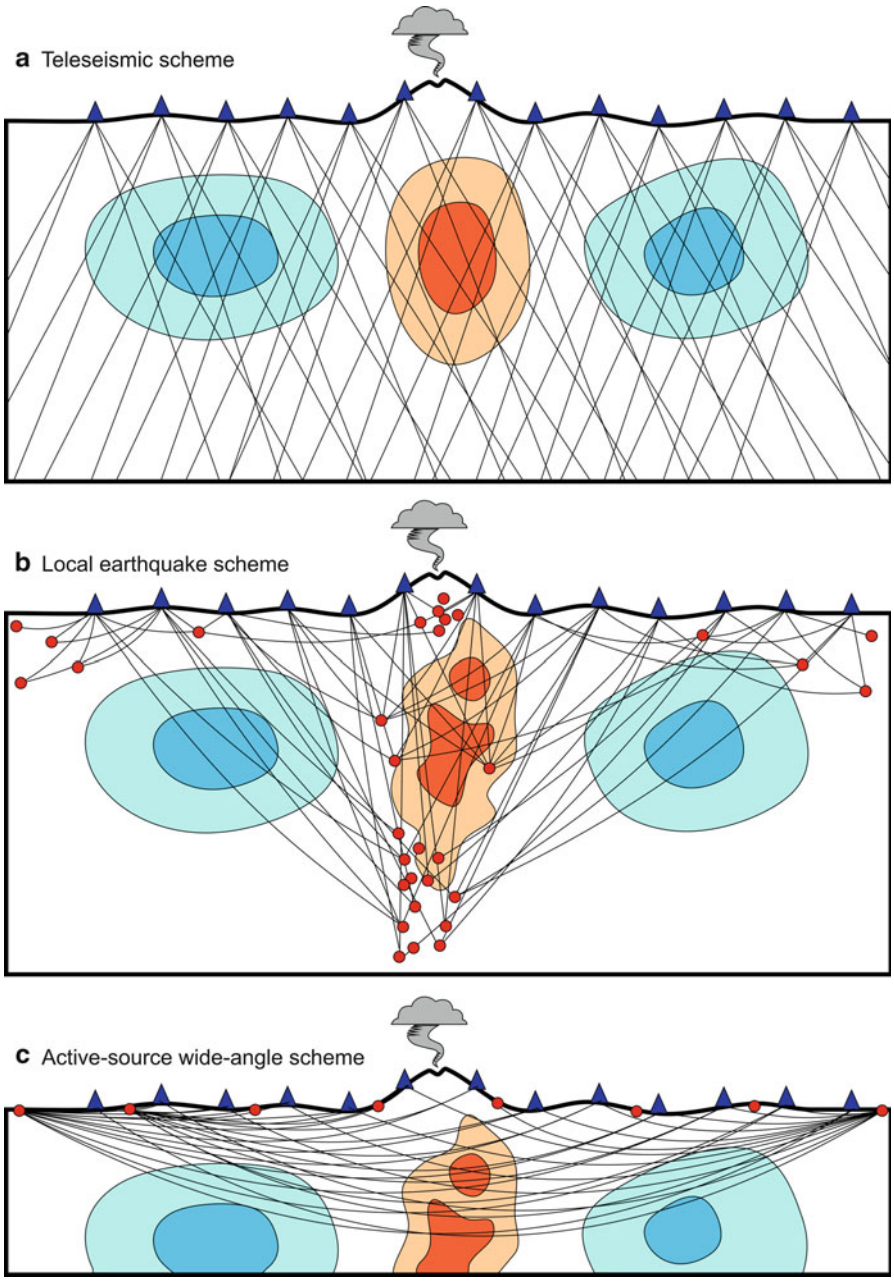

Fig. 1 Observation schemes used in volcano tomography. *Blue triangles* depict seismic stations; *red dots* are sources; *black lines* are seismic rays

not exactly known and must be determined simultaneously with velocity models. This leads to a coupled problem with significant trade-off between velocity and source parameters. However, an important advantage of natural sources compared to the artificial sources is that they are located at some depths which allow illuminating the target object from below at different directions. For many cases, the amount of earthquakes is much larger than that of the artificial explosions. In addition, earthquakes in most cases produce clear P and S waves which can be used for exploring P and S velocities. In turn, both P and S velocities give much more constraints on the petrophysical state of rocks below volcanoes than just a single P model.

DOI 10.1007/978-3-642-36197-5_51-1

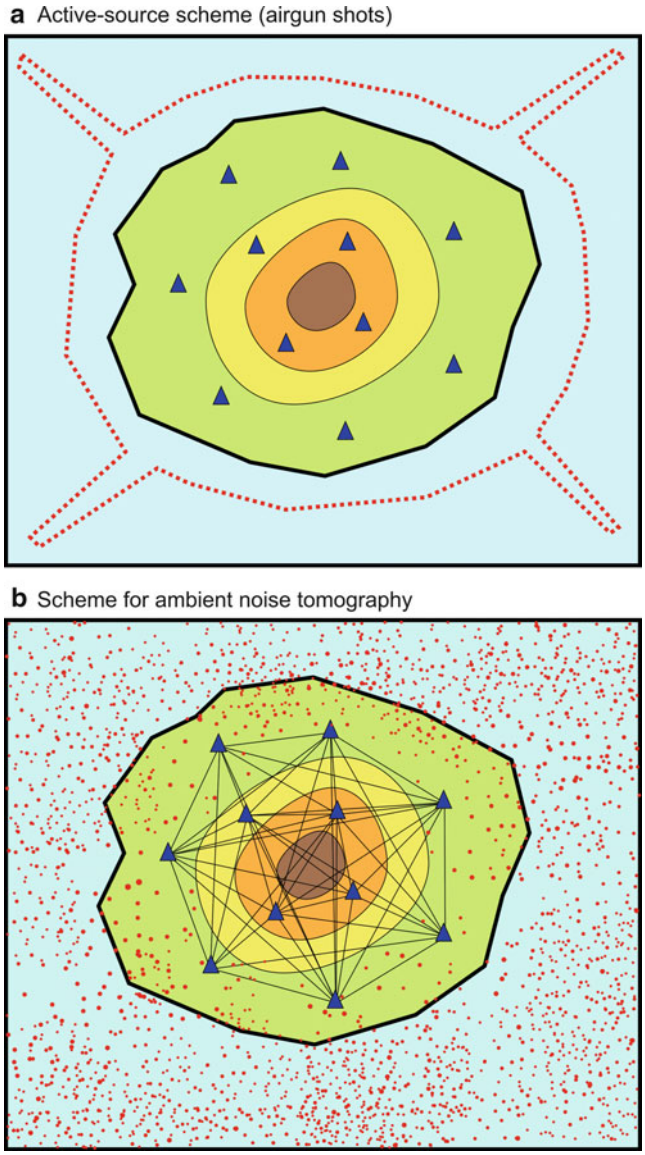

Fig. 2 Schemes for active-source experiments using air-gun shots (**a**) and for ambient noise tomography (**b**). *Blue triangles* depict seismic stations; *red dots* are sources

Ambient Seismic Noise

Ambient seismic noise is the permanent motion of the Earth surface that is not related to earthquakes or specific controlled sources (see also "► Seismic Noise"). When averaged over long time series, this wavefield can be approximately considered as produced by randomly and homogeneously distributed sources (Fig. 2b). Cross-correlation between records of such random wavefields at two stations yields the impulsive response of the media (Green's function) between these two points (e.g., Gouédard et al. 2008). In the present form, every recorder can be converted into a "virtual" source recorded at all other recorders resulting in **N(N-1)/2** source-receiver pairs for a network of **N** stations, as shown in Fig. 2b. Shortcomings of noise-based approach are (1) dependence on noise sources distribution that in many cases is not perfectly homogeneous possibly preventing successful reconstruction of impulsive responses for a part of station pairs; (2) need of long continuous records (months or years); and (3) the fact that reconstructed virtual sources are located at the surface and are dominated by surface waves.

DOI 10.1007/978-3-642-36197-5_51-1

Receivers

Networks for active and passive surveys on volcanoes use generally the same instruments as for similar seismological studies in other regions. Tomography inversion needs numerous stations in a network (more than ten) which are usually deployed temporarily. Such networks consist of portable seismic stations which are composed of three major components: sensor, recorder, and power supply. In some cases, there is also a device for telemetric transition of signal.

Seismic sensor is a kind of "microphone" which converts the ground movements into electric signal. Modern sensors which are used for volcano surveys are three-component broadband instruments which allow recording oscillations of more than 30–40 s period (see also "▶ Broadband Seismometers"). It should be noted that for the body-wave tomography based on local seismicity such broad frequency capacity is not really required: the signal from local earthquakes is clearly seen at frequencies of more than 1Hz.

Seismic recorder is a tool which digitizes the analogue electrical signal coming from the sensor and records it onto a flash or another kind of memory. In each recorder, there should be also a GPS receiver which synchronizes the absolute time. In some cases, sensors and recorders are combined in one unit.

All recorders and most broadband sensors consume the electric power, and an important part of the seismic station is **power supply**. It can include chemical rechargeable or single-used batteries, solar panels, or wind generators. Using each type of power source is determined by the conditions of real experiments. For example, in Kamchatkan volcanoes, solar panels cannot be used due to large amount of snow during the most part of the year. Furthermore, there is a risk of destruction of any part located outside the ground by wild animals or vandals. In this case, an only possibility to conserve the station is to place the station deep into the ground together with batteries.

Some Hints on the Network Design

Design of seismological networks for performing tomography studies has some particular features. Here some hints which should be taken into account while deploying seismic networks are given.

- In case of using refracted rays from active (artificial) sources, when both sources and receivers are located near the surface, a typical depth of seismic ray propagation is 1/10–1/15 of the source-receiver distance (Fig. 1c). Thus, to study the depths of ~10 km beneath the volcano, the sources and receivers should be located in the opposite sizes of the volcano at distances of 50–70 km.
- The spacing between stations normally has the same order as the minimum size of resolved anomalies in the tomographic inversion. Further decrease or increase of the resolution depends on the distribution of events. If there are a very few events, densification of the network would hardly bring to the resolution increase. In contrary, in case of a large amount of sources evenly distributed throughout the study area, the resolved patterns can be smaller than the station spacing.
- For passive sources (local earthquakes), the depth of seismic model resolved from tomographic inversion cannot be larger than the maximum depths of sources.
- For uncontrolled sources (earthquakes), a critical parameter for tomography is a number of picks per events. If this number is equal to 4, one can theoretically locate the sources but cannot get any information about the velocity model. In practice, the data are noisy, and to get a stable location of source, more than four picks are required. The information on the velocity structure can be extracted only if the number of picks is more than 10. The higher this value is, the more velocity parameters can be retrieved and the higher resolution model will be obtained.
- Using out-of-network events (within reasonable limits) can appear to be useful for tomography as was shown by Koulakov (2009b). Although the location accuracy for such events is fairly low, they improve the ray coverage and help in increasing the spatial resolution beneath the network area.

DOI 10.1007/978-3-642-36197-5_51-1

- In all cases, prior the deployment of the network, it is useful to simulate a series of synthetic models with possible configurations of network, sources, and target objects that are expected in the real case. This can help to optimize the distribution of seismic stations in the real experiment.

Seismic Tomography Methods Based on Body Waves

Basic Principle of Body-Wave Seismic Tomography

In the ray-based approach which is used in most body-wave tomography algorithms, seismic waves are produced by point sources. Along this way, seismic rays accumulate the information on the inner structure of the Earth. The purpose of seismic tomography is to decipher this information and to reconstruct the structure inside the Earth. Most simple and most popular way for many practical applications, including volcano tomography, is the kinematic approach based on using travel times of seismic rays. Travel times of seismic rays can be represented as an integral along the ray paths

$$T = \int_{\gamma} \frac{dS}{V(x,y,z)} \tag{1}$$

where γ is the ray path and V is seismic velocity. Here, an infinite frequency of the wave is presumed which allows presenting the ray as a curved line. Actually, this is often not true in seismology where the wavelengths are in some cases compatible with the size of the target objects. For these cases, there are methods of finite-frequency tomography which are based on "fat" rays representing a banana-shaped area having a rather complex sensitivity patterns (e.g., Husen and Kissling 2001). Although there are some successful applications of this method in global or in teleseismic tomography (Montelli et al. 2004), it was not yet widely implemented for volcano tomography. Up to today, most of the practical applications for studying the volcanoes are based on the ray-based kinematic approach.

In general, the velocity field in Eq. 1 is a function which is represented by infinite number of mathematical points. In practice, to solve the inverse problem, i.e., to derive velocity distribution based on given travel times, the velocity field should be parameterized with a finite number of parameters. There are different methods of parameterization, such as using regular or irregular cells, nodes with linear interpolation, harmonic functions with unknown coefficients, etc.

Another problem of solving the inverse problem based on the representation in Eq. 1 is that this problem is nonlinear. It means that one should find the velocity distribution based on the ray paths which are strongly affected by the unknown velocity distribution. The direct solution of this nonlinear problem is almost never used for practical applications. Actually, in most cases, this problem is reduced to the linear representation. It is assumed that the unknown velocity distribution is close to the given reference model, and in this case, the problem in Eq. 1 is reduced to the linear integral

$$\Delta t = -\int_{\gamma_0} \frac{\Delta v\, dS}{V_0^2(x,y,z)} \tag{2}$$

where Δv is unknown velocity anomalies, Δt is time residuals, $V_0{}^2$ is velocity in the reference model, and γ_0 is the ray path in the given reference model. Then, the continuous representation in Eq. 2 can be reduced into the discrete system of linear equations:

DOI 10.1007/978-3-642-36197-5_51-1

$$\Delta t_i = \sum_j A_{ij} \Delta v_j \tag{3}$$

where Δv is the unknown value of jth velocity parameter and A_{ij} is the first-derivative matrix which represents an effect of a unit velocity change of jth parameter on travel time ith ray. In the case of cell parameterization, each element of this matrix is just the length of jth ray in ith cell. In the case of uncontrolled sources, this matrix also includes the elements for relocation of sources (four parameters, *dx, dy, dz*, and *dt*, for each source). In practical tomography studies, where this matrix may appear to be very large, the system in Eq. 3 is solved using the iterative LSQR algorithm (Paige and Saunders 1982) which proceeds only nonzero elements in the matrix and performs the calculations line by line without keeping the entire matrix in the memory. The direct solving of the system as it stands in Eq. 3 normally fails because of strong instability of the solution due to noise in the data. To avoid this problem, the inversion should be regularized using some additional terms. The most popular way of regularization is the amplitude damping which is realized by adding a diagonal matrix block with zero data vector. Another way is damping a gradient between all pairs of neighboring parameters (nodes or cells) that allows controlling the smoothness of the solution.

The quality of the solution and optimal values of the inversion parameters are estimated based on synthetic modeling which should simulate the conditions of a real experiment as close as possible. The synthetic travel times are computed in an artificial model and perturbed by a realistic noise. Then, the model parameters are "forgotten," and the reconstruction procedure is performed identically as in the case of observed data processing. This step is especially important for the volcano tomography where the distributions of sources and events are often far from optimal.

There are different seismic tomography schemes which are used for different purposes in geosciences. Many of them are used for studying the volcano feeding systems on scales from the entire mantle (thousands kilometers) to the uppermost layers (hundreds meters) (e.g., Koulakov 2013). Here, only some examples of tomography studies on scales from first to dozens kilometers are given. They provide the information about magma sources in the crust and uppermost mantle that are directly responsible for eruptions of active volcanoes.

Teleseismic Tomography

Seismic tomography is a relatively young method which started actively developed from the late seventies after the pioneer work by Aki et al. (1977). The method proposed in this study is called **teleseismic tomography**, and it uses the relative time delays from distant (teleseismic) earthquakes recorded by seismic stations located in the study area (Fig. 1a). There were several attempts of using this method for studying the volcanoes. For example, Ellsworth and Koyanagi (1977) have implemented the teleseismic scheme for studying the crustal structure beneath Kilauea volcano in Hawaii. Three years later, Sharp et al. (1980) have published the tomographic model for Mt. Etna. Among later studies, one can mention the work by Stauber et al. (1988) who presented tomographic models of Newberry Volcano, Oregon, based on teleseismic delays.

It should be noted that during the last decades, the teleseismic tomography is almost not used anymore for studies of crustal structures beneath volcanoes because of several reasons. The first problem is that nearly vertical seismic rays in the study area cause poor vertical resolution which leads to strong vertical smearing of the retrieved anomalies. Another problem, which seems to be more serious, is related to the fact that the teleseismic waves are usually of low frequency (around 1 Hz and lower). Thus, the large wavelengths strongly limit the resolution capacity of this method. Theoretically, it cannot provide robust images of anomalies smaller than 8–15 km. Magma reservoirs are usually expected to be smaller in size, and thus, they are hardly resolvable by teleseismic tomography.

DOI 10.1007/978-3-642-36197-5_51-1

Local Earthquake Tomography

Another method, which is called **local earthquake tomography (LET)**, uses the data of arrival times of P and S waves from earthquakes located within the study area or slightly outside (Fig. 1b). Because of using the uncontrolled sources, the solution in this case is reduced to the coupled problem of simultaneous determination of source parameters and velocity models. Active volcanoes usually produce a lot of seismicity related to processes in magmatic reservoirs and tectonic displacements in the crust. Therefore, deploying stations for the LET experiment is much cheaper than organizing active-source works with the use of explosions or air-gun shots. Furthermore, the earthquakes in passive source schemes are distributed at some depths that enable much more favorable observation system than in the case of active-source studies. In addition, seismic records from earthquakes usually provide the data on P and S waves that allows getting more information on petrophysical state of rocks in volcanoes than just a single P-velocity model which is usually resulted from the active-source studies. The problem of LET studies is an uncontrolled distribution of sources which is not always optimal to get optimal ray coverage in the target areas. An important difficulty of LET is the uncertainty of the source locations and the trade-off between source and velocity parameters. Another technical problem of LET is the necessity of fairly long deployment of a large number of seismic stations (for more than several months) which is required to accumulate sufficient information on the seismicity in the volcano area. This needs solving some logistical issues related to providing power supply and hiding the equipment.

The first LET algorithm was developed and implemented to real seismological data by Thurber (1983). One year later, the same algorithm was used for studying the crustal structure beneath Kilauea volcano (Thurber 1984). Among the later studies based on this approach, one can single out the studies of Hengill-Grensdalur volcanic complex in Iceland (Foulger and Toomey 1989) and of Mount St. Helens (Lees 1992). There are more than ten different LET studies of Mt. Etna which appears to be one of the best studied volcanoes in the world (e.g., Villasegnor et al. 1998; Chiarabba et al. 2000; Patane et al. 2006). Note that the work by Patane et al. (2006) was a pioneer study presenting the 4D tomography model which revealed temporal variations of seismic structure beneath the volcano having possible relations to the eruption activity (see also "► Seismic Monitoring of Volcanoes"). During the last decades, the LET methods have become the most popular for studying crustal structure beneath volcanoes. Nowadays, there are dozens of successful studies of volcanoes in different parts of the world. In the final part of this paper, two examples of recent studies of Mt. Spurr in Alaska (Koulakov et al. 2013a) and of Klyuchevskoy volcano group in Kamchatka (Koulakov et al. 2011, 2013b) will be presented. Both of these studies were performed using the LET code LOTOS (Koulakov 2009a).

Studies with Human-Made Sources

Human-made sources or active sources are used in many seismic studies of volcanoes. The first experiments of three-dimensional active-source investigations of volcanoes were made in two relict calderas located in the Cascade Range, western USA. One of them is the potentially active Newberry shield volcano with the caldera of ~8 km diameter. In the active seismic experiment, Achaer et al. (1988) used three chemical explosions and a dense receiver network covering the caldera. They obtained a rather clear low-velocity anomaly at about 3 km depth which was interpreted as a magma chamber. Another study was made in the same year in the Medicine Lake Caldera by Evans and Zucca (1988). They deployed 120 seismometers and made eight chemical explosions which were recorded by all stations. The tomography inversion of travel time data revealed a low-velocity pattern beneath the caldera which was also interpreted as a magma source.

Performing 3D experiments using onshore explosions appeared too expensive and not providing sufficient spatial resolution with the available number of explosions. Therefore, many onshore experiments were mostly organized along one or several profiles (Fig. 1c). For example, Zollo et al. (1996) used

DOI 10.1007/978-3-642-36197-5_51-1

four chemical explosions on a profile passing through the summit of the Vesuvius volcano (Italy). Their P-velocity model reveals a rather clear high-velocity anomaly beneath the volcano. A similar experiment, but with five explosions on two crossing profiles, was performed by Aoki et al. (2009) for the Asama volcano in Japan. Similarly, as in the previous case, they found a clear high-velocity body beneath the volcano.

It should be noted that logistically the experiments based on chemical explosions are very difficult. Because of high expenses, the number of shots is strictly limited that makes it problematic to illuminate the target objects from different directions. Furthermore, the 2D approximations are often too rough for the volcanic areas where the expected structures are strongly 3D. In addition, the explosion type sources are not ecologically safe, and in most volcanic areas, they are prohibited now.

Good solutions for areas which are close to the seashore are the underwater air-gun shots which can be used to generate high-quality and sufficiently powerful seismic signal and can surround the target area (Fig. 2a). Nowadays, this scheme is widely used in experiments in many volcanic areas. Among many different studies, three examples are selected here:

- A very interesting site for seismic investigations is the volcanic Deception Island in Antarctic which was studied by Zandomeneghi et al. (2009). This island has a circular shape and is suitable for performing air-gun shots inside and outside the circle. Using onshore and offshore seismometers made this observation system suitable for high-resolution tomography studies. The inversion of travel time data revealed the seismic structures down to ∼2 km which appeared to be linked with the main geological structures. The circular rim of the caldera is associated with high-velocity lineaments. Inside the caldera, a low-velocity anomaly is observed.
- A network with onshore and offshore stations and 4,414 air-gun shots were used by Paulato et al. (2010) to build a tomographic model beneath Montserrat Island in Lesser Antilles. They found that the location of the Island is associated with high P velocity. Especially sharp positive anomaly is located beneath the Soufriere volcano.
- The high-resolution 3D structure beneath the Tenerife Island was studied by Garcia-Yeguas et al. (2012) based on a large amount of air-gun shots and fairly dense onshore seismic network consisting of 140 stations. The main volcanic structure of the Las Cañadas-Teide-Pico Viejo Complex (CTPVC) is characterized by a high P-wave velocity body, similar to many other stratovolcanoes. Furthermore, reduced P-wave velocities are found in a small confined region in CTPVC and are more likely related to hydrothermal alteration, as indicated by the existence of fumaroles.

Imaging and Monitoring of Volcanoes Based on Ambient Seismic Noise

General Principle, Data Processing, and Inversion Approaches

New methods for probing the Earth's interior using noise records only emerged during the last decade (e.g., Campillo et al. 2011). Origin of seismic noise strongly depends on the considered spectral range (see also "► Seismic Noise"). At high frequencies (>1Hz), the noise is strongly dominated by local sources that are often related to strong winds or the anthropogenic activity. Seismic noise at intermediate periods (between 1 and 20 s) that is most often used for studies of volcanoes is dominated by natural sources. In particular, the two main picks in the seismic noise spectra in this so-called microseismic band (1–20 s) are related to forcing from oceanic gravity waves. The interaction between these oceanic waves and the solid Earth is governed by a complex nonlinear mechanism (Longuet-Higgins 1950), and the noise excitation depends on many factors such as the intensity of the oceanic waves but also the intensity of their interferences as well as the seafloor topography. Overall, the generation of seismic noise is expected to

DOI 10.1007/978-3-642-36197-5_51-1

be strongly modulated by strong oceanic storms and, therefore, to have a clear seasonal and nonrandom pattern. However, when averaged over long time series, distribution of sources of microseismic noise can be approximated as random and homogeneous. In this case, cross-correlation of noise records between two stations yields the impulsive response (Green's function) between these two points (e.g., Gouédard et al. 2008). In the case of a uniform spatial distribution of noise sources, the cross-correlation of noise records converges to the complete Green's function of the medium, including all reflection, scattering, and propagation modes. However, in the case of the Earth, most of ambient seismic noise is generated by atmospheric and oceanic forcing at the surface. Therefore, the surface-wave part of the Green's function is most easily extracted from the noise cross-correlations.

Seismic surface waves, in contrast with body waves, are waves that propagate in a waveguide near the Earth's surface. There are two types of **surface waves**: **Rayleigh** (vertically polarized waves) and **Love** (horizontally polarized waves transverse to the direction of motion). Their depth sensitivity depends on frequency, with a fair approximation being about a third of a wavelength. As a result, the surface waves are strongly dispersive with longer periods (wavelengths) propagating faster than shorter periods because of the general increase of seismic speed with depth in the Earth.

Using surface waves extracted from correlations of seismic noise for imaging of the Earth's interior is called **ambient noise surface-wave tomography**. This approach generally consists of three steps (e.g., Ritzwoller et al. 2011). First, noise cross-correlations between every pair of stations in the array are computed, and interstation phase or group travel times as a function of period are measured from the resulting waveforms. Second, two-dimensional maps of the speed of Rayleigh or Love waves as a function of frequency are produced. At the last step, these maps are inverted for a 3D distribution of shear speeds.

Applications of Ambient Noise Seismic Tomography (ANST) to Studies of Volcanoes

After recent emergence of the ambient noise surface-wave tomography (e.g., Shapiro et al. 2005), it became clear that this method might be very useful for studying structures within volcanoes because of its relatively low coast (especially comparing with active-source studies) and because of good coverage of the shallow part of edifices compared with earthquake-based body-wave imaging. First "volcanic" application of ANST was performed at Piton de la Fournaise located at La Réunion Island (Brenguier et al. 2007). This hot-spot volcano is very active with on average more than one eruption per year during the past two centuries. The noise-based tomography was based on correlations of 18 months of records by 21 short-period vertical-component stations of the permanent volcano monitoring network. Rayleigh wave group velocities could be measured between 2 and 5 s of period. Inversion of these dispersion curves resulted in a shear velocity model extending between the surface and the depth of 1 km below sea level (while average elevation of the volcano is $\sim$2 km). The main result of this study was imaging of an intrusive high-velocity body below the main crater moving westward from the surface to 1 km below sea level. This body is located above the shallow magma reservoir and coincides with the region through which the magma ascends during the summit eruptions.

Following the pioneering study of Brenguier et al. (2007), the ANST was applied to image subduction zone volcanoes: Okmok in Aleutian Islands (Masterlark et al. 2010), Lake Toba in Sumatra (Stankiewicz et al. 2010), and Asama in Japan (Nagaoka et al. 2012). The first study used 12 stations from a permanent monitoring network, and the second study used 40 stations from a temporary deployment, while the third study used 81 sensors combined from permanent and temporary networks. In all these studies, the authors reported very similar results: imaging of low-velocity anomalies corresponding to magma reservoirs at depths below 4 km.

DOI 10.1007/978-3-642-36197-5_51-1

Noise-Based Volcano Monitoring

One of the advantages of using continuous seismic noise records to characterize the earth materials is that a measurement can easily be repeated (see also "► Seismic Monitoring of Volcanoes"). First application of this idea to volcano monitoring was done by Sens-Schönfelder and Wegler (2006) who used the repetitive waveforms of seismic noise cross-correlations to track changes in the subsurface material properties on mount Merapi in Indonesia during 2 years. This study was based on high-frequency (>1 Hz) waves and mainly revealed seasonal variations caused by changes of hydrological conditions in a very shallow layer. Brenguier et al. (2008) used noise cross-correlations at intermediate periods (between 1 and 10 s) to detect decreases in seismic velocity a few weeks before eruptions that suggests preeruptive inflation of the volcanic edifice of the Piton de la Fournaise. A comprehensive review of recent advancements in the noise-based volcano monitoring is provided by Brenguier et al. (2011) (see also "► Tracking Changes in Volcanic Systems with Seismic Interferometry").

Current Limitations and Prospective

Application of seismic noise cross-correlation methods for studies of volcanoes is a rapidly growing field. However, these methods have some important limitations that are mainly related to the properties of the seismic noise recorded at the Earth surface. So far, the basic theoretical foundation of the cross-correlation method assumes a random and homogeneous distribution of the wavefield sources, while properties of a real seismic noise may deviate from this simplified model. This implies that applications of the noise-based imaging or monitoring should be accompanied by studies of properties of recorded seismic noise to characterize the degree of its spatial and temporal inhomogeneity and to determine the minimal time required for good convergence of noise cross-correlations. Development of advanced methods for the preprocessing of the noise time series in order to improve the quality of the extracted signals and to decrease the convergence time is a very active research area.

Up to date, the noise-based seismic tomography was based on surface waves that are most easily extracted from noise cross-correlations but have a limited resolution in deep layers. Most recent results demonstrate that, when working with large and dense arrays of seismometers, it is possible to indentify body waves in correlation waveforms and to measure their travel times (e.g., Boué et al. 2013; Lin et al. 2013). This gives a hope that noise-based body-wave tomography of volcanoes could be developed in the future.

Examples of Tomography Studies of Volcanoes

Tomography of Mt. Spurr

Mount Spurr is an active predominantly andesitic volcano in Alaska located at the northeastern end of the Aleutian arc. Before a single eruption in 1953, it was considered as a dormant volcano. In 1992, a series of three explosive eruptive events occurred on June 27, August 18, and September 16–17 in a small composite cone forming the Crater Peak on the south flank of Mount Spurr. The structure beneath Mt. Spurr in a period of time nearly corresponding to this eruption was studied by Power et al. (1998) using the data collected from 1991 to 1993 by 7–11 seismic stations of the Alaska Volcano Observatory (AVO).

The most recent episode of Mt. Spurr unrest occurred in 2004–2006 which accompanied with strong seismicity and fumarolic activity. However, this episode did not result at any magma eruption, and thus, it was called as "lost eruption." For 1 month in June 2005 corresponding to the middle stage of this unrest, the AVO deployed a fairly dense seismic network consisting of 26 broadband three-component stations which operated in addition to 11 short-period stations of the permanent network. During this period,

DOI 10.1007/978-3-642-36197-5_51-1

512 crustal earthquakes were located in the area of Mt. Spurr using P and S picks recorded by portable and permanent stations. The final catalog contained 5,960 P- and 4,973 S-wave arrival times with an average of 20 picks per event. These data were used to perform the tomographic inversion presented in Koulakov et al. (2013a).

The result of tomographic inversion including the 3D distributions of P and S velocities, Vp/Vs ratio, and accurate source locations is presented in Fig. 3. The horizontal section at 5 km depth demonstrates a prominent anomaly of high Vp/Vs ratio which reaches the value of 1.9 located beneath the northern rim of the volcano. This pattern coincides with the distribution of shallow seismicity. In the deeper section at 22 km depth, this anomaly is located at the same place, but it appears to be less intensive than another zone of high Vp/Vs ratio which is collocated with a cluster of deep crustal earthquakes. In vertical section, these two anomalies look like two fingers of high Vp/Vs ratio separated by 8 km of lateral distance. One of the two anomalies nearly reaches sea level beneath the northern border of the caldera, but is separated from the surface with a zone of low Vp/Vs ratio. The top of the second anomaly appears to be much deeper and may reach a depth of 20 km. The earthquakes that occurred during the 3-month span show distinct clusters near the tops of each of these fingers which support the active behavior of these structures. It is important that for both these finger-shaped anomalies, the high Vp/Vs correspond to higher P and lower S velocities.

The observed finger-like features are suggestive of pathways through the crust and possibly correspond to complexes of conduits that transport liquid volatiles and/or melts from the mantle. The combination of high Vp and low Vs suggests the presence of liquid fluids and/or melts and the rock composition corresponding to the low crustal or even mantle levels. The existence of very low values of Vp/Vs above the NW anomaly might be an indicative for aggregate transition occurred between the top of the plume and the surface. It is important that the NW finger location generally coincides with the presence of fumaroles and active volatile flux during the most recent eruption in 2004–2005. It can be proposed that this liquid fluids brought by the NW conduit are transformed to gases at shallow depths which can escape to the surface without producing any stresses. This explains lack of any explosive activity in this location during the 2004–2005 unrest of Mt. Spurr (Fig. 3).

Another conduit located below the Crater Peak seems to be blocked at ~20 km depth. This fact is supported by the occurrence of deep seismicity just above this anomaly. In this blocked channel, the accumulation of high pressure is more probable which makes it more dangerous for a potential explosive eruption. Note that the explosive eruption of Mt. Spurr in the SE rim in 1992 occurred just above this anomaly.

Tomography of the Klyuchevskoy Volcano Group

The Klyuchevskoy volcano group is located in Kamchatka, in the far east of Russia. It includes 13 active and dormant volcanoes of various types and compositions located in a relatively small area of approximately 100 × 60 km. The main volcano of the group, Klyuchevskoy Sopka, has the elevation of ~4,800 m, and it is the highest volcano in continental Eurasia. Another volcano of the group, Bezymianny, located at approximately 10 km distance from the Klyuchevskoy volcano is an explosive-type andesitic volcano. One of the world's largest explosive eruptions in the twentieth century occurred here in 1957. The Tolbachik complex is situated in the southwestern part of the Klyuchevskoy group, and it consists of several shield and stratovolcanoes of predominantly basaltic compositions. Plosky Tolbachik, which is currently active, is a typical Hawaiian-type volcano with fissure eruptions and calderas. The existence of so many different volcanoes located close to each other can most likely be explained by complex processes of fractioning, mixing, and melting in magmatic reservoirs located under the volcanic group at different depth levels.

During the last several decades, the volcano-related seismicity in the Klyuchevskoy group has been monitored by the Kamchatkan Branch of Geophysical Survey. After 1999, a network consisting of

DOI 10.1007/978-3-642-36197-5_51-1

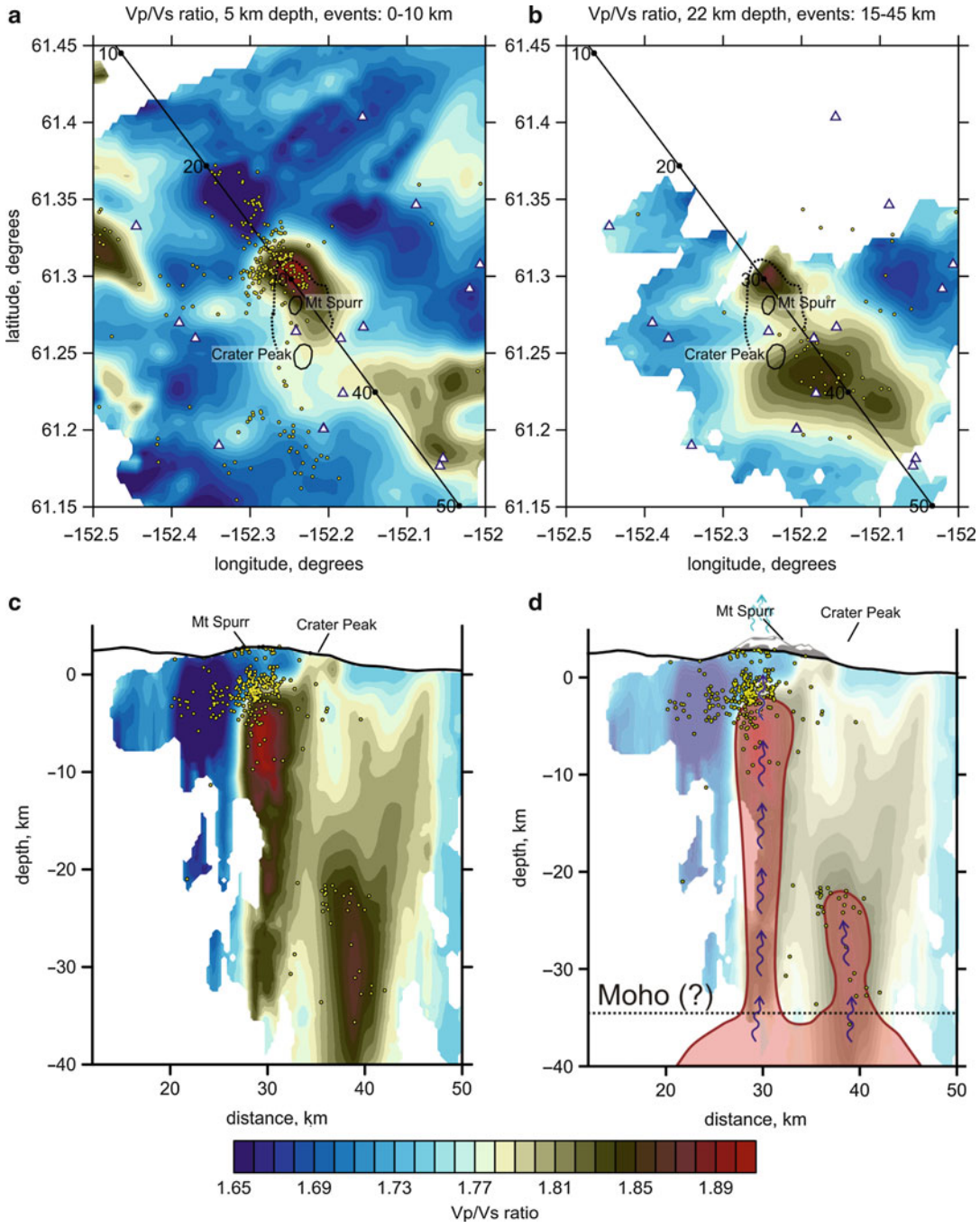

Fig. 3 Distribution of the Vp/Vs ratio in two horizontal and one vertical section. *Dotted line* depicts the limits of the caldera rim. *Triangles* indicate the locations of stations. *Yellow dots* mark the source locations. *Bottom-right plot* represents the interpretation of the results. *Blue waved arrows* indicate hypothetical migration of fluids and their escape to the atmosphere in 2004–2006 unrest (Reproduced from Koulakov et al. 2013a, JRL)

17 digital telemetric stations was installed in the region of the Klyuchevskoy group. From 1999 to 2009, it provided the information on more than 80 thousand events and the corresponding half million of P and S arrival times. The tomographic inversions were performed based on selected yearly subsets. The temporal variations of seismic structure are especially interesting in the context of the volcanic activity during the considered time. In particular, in 2005, there were simultaneous eruptions of the Klyuchevskoy and

DOI 10.1007/978-3-642-36197-5_51-1

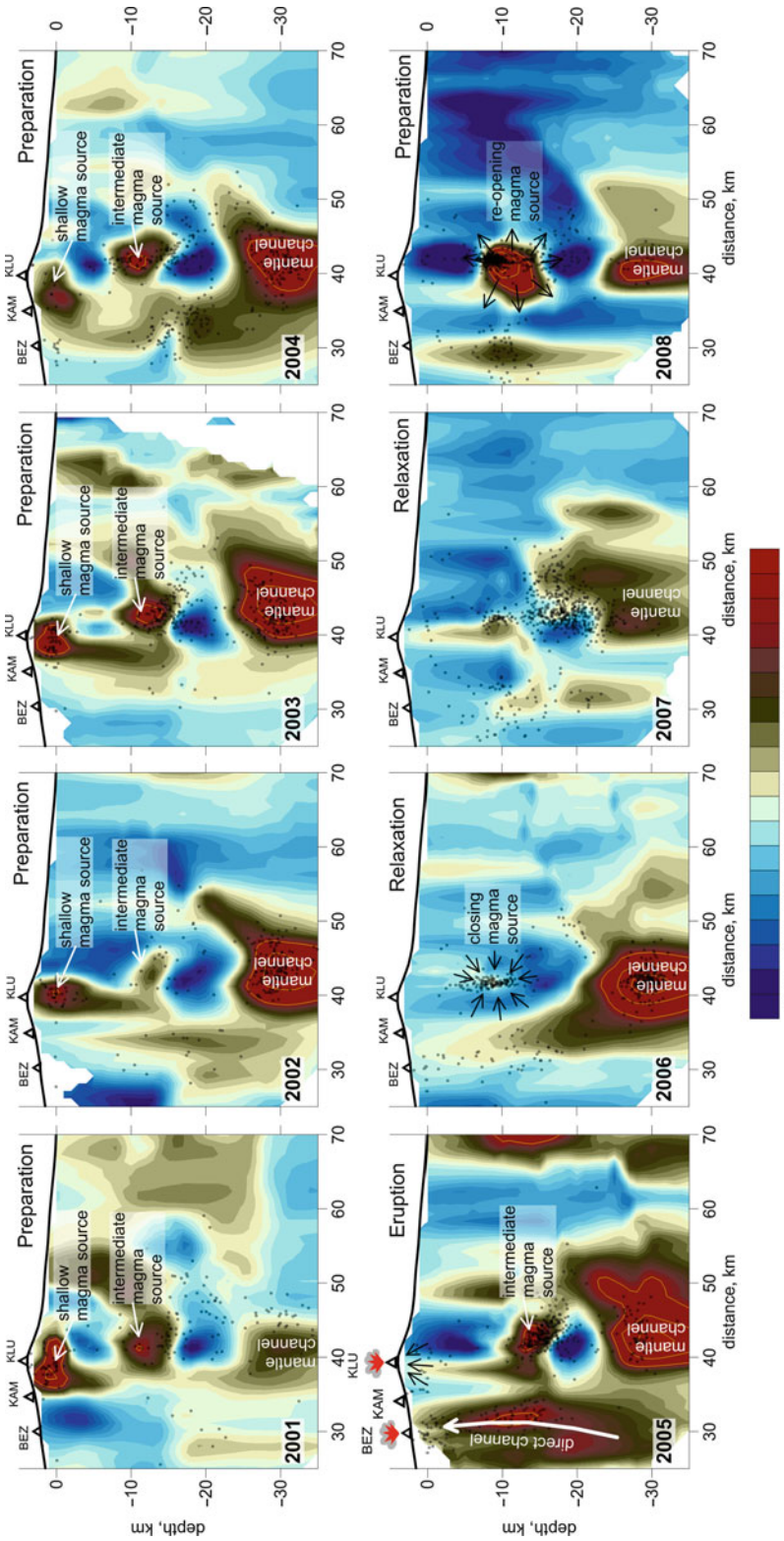

Fig. 4 Cross sections of Vp/Vs from tomographic inversions for each year from 2001 to 2008 for a profile passing through Klyuchevskoy (KLU) and Bezymianny (BEZ) volcanoes. In areas of high Vp/Vs ratios, yellow lines show contours of Vp/Vs = 2.0, 2.1, and 2.2. *Dots* show earthquakes less than 0.5 km from the profile, and triangles mark the locations of the volcanoes near the profile. The eruptions of Klyuchevskoy and Bezymianny volcanoes in 2005 are highlighted. The main phases and structural elements, which are discussed in the text, are indicated (Reproduced from Koulakov 2013, JVGR)

DOI 10.1007/978-3-642-36197-5_51-1

Bezymianny volcanoes that give a possibility to explore the changes of the crust related to the volcanic activity at stages of preparation, activation, and relaxation (see also "► Seismic Monitoring of Volcanoes").

The results of tomographic inversion corresponding to the year 2004 just before the activation phase were presented in a separate study by Koulakov et al. (2011). Similar structures are observed in the precedent 2003 year (Koulakov 2013). The key feature of these models is a strong anomaly of a high Vp/Vs ratio, reaching values of 2.2, located below 25 km depth. Within this anomaly, the P velocity appears to be higher than average, whereas the S velocity is strongly low. This combination of seismic anomalies is a possible indicator for a mantle conduit beneath the Klyuchevskoy group with rocks brought from deep levels and high content of fluids and melts. It was proposed that this conduit is the original magma source that feeds all of the volcanoes in the Klyuchevskoy group.

The tomography result corresponding to 2004 reveals complex contrasted structures in the crust which can be associated with magma sources. The distributions of high values of Vp/Vs ratio reveal at least two levels of magma sources in the crust: one is located at a depth of 10–12 km and another is just below the Klyuchevskoy volcano close to the surface. This may explain the diversity of the volcanic styles in the group. The distribution of earthquakes appears to link different levels of magma storage that may trace the paths of magma migration.

Time variations of seismic structure beneath the Klyuchevskoy group in a time period from 1999 to 2009 were studied by Koulakov et al. (2013b) and presented in Fig. 4. A common feature which is seen in all yearly windows is the anomaly with an extremely high Vp/Vs ratio located below 25 km depth, which was previously mentioned for the year 2004 and interpreted as a mantle conduit feeding all volcanoes of the group. For the crust, this study demonstrates considerable temporal changes of seismic structures. In particular, prior the 2005 eruptions of the Klyuchevskoy and Bezymianny volcanoes, the seismic structures in the crust look generally similar and contain two anomalies of high Vp/Vs ratio beneath the Klyuchevskoy volcano at a depth of 10–12 km and close to the surface. As mentioned above, these anomalies are interpreted as two levels of magma sources. In 2005, the average value of the Vp/Vs ratio increases, and it may be explained by a considerable increase of the fluid and melt content in the crust. In this year, a strong anomaly of high Vp/Vs ratio is observed beneath the Bezymianny volcano, and it appears to link the volcano with mantle sources. In other years, this anomaly was not observed. The shallow anomaly of high Vp/Vs anomaly, which was previously observed beneath the Klyuchevskoy volcano, disappears in 2005. The deeper anomaly at 10–12 km depth is still presented. In the years after the eruption, 2006 and 2007, the average Vp/Vs ratio lowers, and all the patterns at 10–12 km depth that were interpreted as intermediate magma sources in the crust are not observed anymore. Three years later, in 2008, a similar anomaly at the same location starts reappearing again.

The observed variations of the seismic properties are probably related to changes in the stress and deformation fields, migration of fluids, and aggregate transformations in the crust. The mantle conduit, which is visible as an anomaly of high Vp/Vs ratio below 25 km depth at all time periods, should have strong mechanical, thermal, and/or chemical influence upon the bottom of the crust and cause strong seismicity. These stresses lead to the origin of fractures and upward penetration of the fluids to the crust. Reaching intermediate levels, these fluids lead to melting of the overheated rocks. Due to decompression, some of the fluids are transformed to gases that increase the pressure and cause additional fractures. These avalanche-type processes finally lead to the eruptions. During the eruption, most of the fluids escape to the atmosphere, and it causes a decrease in the melt content in the intermediate magma sources in the post-eruption period. Several years later, a new portion of fluids comes from the mantle conduit, and melting of rocks in intermediate reservoirs starts again. An important conclusion that can be drawn from the 4D tomography study is that the magmatic sources appear to be dynamic systems with rapidly variable properties. According to this concept, the magma sources are composed of sponge-type materials with the

capacity to change the proportion of the molten partition depending on the presence of fluids. Propagation of cracks and fluids may occur rather rapidly, and this may abruptly change the properties of the "sponge" material over a period of years or even months or weeks.

Summary

This paper presents an overview with the description of several seismic tomography schemes which are used for studying volcanoes. It describes several examples of practical works including two featured case studies of Mt. Spurr and Klyuchevskoy volcano group. It was demonstrated that seismic tomography gives rich material which allows better understanding of the behavior of magmatic systems. A variety of the tomographic solutions show that there is no uniform structure: each volcano has some particular features and appears to be unique.

During the last years, there appear more and more dense networks on different volcanoes of the world designed for passive and active experiments. There are also new algorithms actively developed during the last years, such as scattering tomography or full waveform inversion, which might appear very effective for studying volcanoes. This gives a hope that increasing amount of data and implementing new algorithms will lead in the nearest time to a real breakthrough in understanding the causes of volcanic activity.

Acknowledgments

The contribution of Ivan Koulakov is supported by the Russian Scientific Foundation (grant #14-17-00430).

References

Achauer U, Evans JR, Stauber DA (1988) High-resolution seismic tomography of compressional wave velocity structure at Newberry Volcano, Oregon Cascade Range. J Geophys Res Solid Earth (1978–2012) 93(B9):10135–10147

Aki K, Christoffersson A, Husebye ES (1977) Determination of the three-dimensional seismic structure of the lithosphere. J Geophys Res 82(2):277–296

Aoki Y, Takeo M, Aoyama H, Fujimatsu J, Matsumoto S, Miyamachi H, Yamawaki T (2009) P-wave velocity structure beneath Asama Volcano, Japan, inferred from active source seismic experiment. J Volcanol Geotherm Res 187(3):272–277

Boué P, Poli P, Campillo M, Pedersen H, Briand X, Roux P (2013) Teleseismic correlations of ambient seismic noise for deep global imaging of the. Earth Geophys J Int 194(2):844–848. doi:10.1093/gji/ggt160

Brenguier F, Shapiro NM, Campillo M, Nercessian A, Ferrazzini V (2007) 3-D surface wave tomography of the Piton de la Fournaise volcano using seismic noise correlations. Geophys Res Lett 34:L02305. doi:10.1029/2006GL028586

Brenguier F, Shapiro N, Campillo M, Ferrazzini V, Duputel Z, Coutant O, Nercessian A (2008) Toward forecasting volcanic eruptions using seismic noise. Nat Geosci 1(2):126–130

Brenguier F, Clarke D, Aoki Y, Shapiro NM, Campillo M, Ferrazzini V (2011) Monitoring volcanoes using seismic noise correlations. C R Geosci 343:633–638. doi:10.1016/j.crte.2010.12.010

DOI 10.1007/978-3-642-36197-5_51-1

Campillo M, Roux P, Shapiro NM (2011) Correlations of seismic ambient noise to image and to monitor the Solid Earth. In: Gupta HK (ed) Encyclopedia of solid earth geophysics. Springer, Dordrecht, pp 1230–1235

Chiarabba C, Amato A, Boschi E, Barberi F (2000) Recent seismicity and tomographic modeling of the Mount Etna plumbing system. J Geophys Res Solid Earth (1978–2012) 105(B5):10923–10938

Ellsworth WL, Koyanagi RY (1977) Three-dimensional crust and mantle structure of Kilauea Volcano, Hawaii. J Geophys Res 82(33):5379–5394

Evans JR, Zucca JJ (1988) Active high−resolution seismic tomography of compressional wave velocity and attenuation structure at Medicine Lake Volcano, Northern California Cascade Range. J Geophys Res Solid Earth (1978–2012) 93(B12):15016–15036

Foulger GR, Toomey DR (1989) Structure and evolution of the Hengill-Grensdalur Volcanic Complex, Iceland: geology, geophysics, and seismic tomography. J Geophys Res Solid Earth (1978–2012) 94(B12):17511–17522

García-Yeguas A, Koulakov I, Ibáñez JM, Rietbrock A (2012) High resolution 3D P wave velocity structure beneath Tenerife Island (Canary Islands, Spain) based on tomographic inversion of active-source data. J Geophys Res 117, B09309, doi:10.1029/2011JB008970

Gouédard P, Stehly L, Brenguier F, Campillo M, Colin de Verdière Y, Larose E, Margerin L, Roux P, Sanchez-Sesma FJ, Shapiro NM, Weaver RL (2008) Cross-correlation of random fields: mathematical approach and applications. Geophys Prospect 56:375–393

Husen S, Kissling E (2001) Local earthquake tomography between rays and waves: fat ray tomography. Phys Earth Planet In 123(2):127–147

Koulakov I (2009a) LOTOS code for local earthquake tomographic inversion. Benchmarks for testing tomographic algorithms. Bull Seismol Soc Am 99(1):194–214. doi:10.1785/0120080013

Koulakov I (2009b) Out-of-network events can be of great importance for improving results of local earthquake tomography. Bull Seismol Soc Am 99(4):2556–2563. doi:10.1785/0120080365

Koulakov I (2013) Studying deep sources of volcanism using multiscale seismic tomography. J Volcanol Geotherm Res 257:205–226. doi:10.1016/j.jvolgeores.2013.03.012

Koulakov I, Gordeev EI, Dobretsov NL, Vernikovsky VA, Senyukov S, Jakovlev A (2011) Feeding volcanoes of the Klyuchevskoy group from the results of local earthquake tomography. Geophys Res Lett 38:L09305. doi:10.1029/2011GL046957

Koulakov I, West M, Izbekov P (2013a) Fluid ascent during the 2004–2005 unrest at Mt. Spurr inferred from seismic tomography. Geophys Res Lett. doi:10.1002/grl.50674.

Koulakov I, Gordeev EI, Dobretsov NL, Vernikovsky VA, Senyukov S, Jakovlev A, Jaxybulatov K (2013b) Rapid changes in magma storage beneath the Klyuchevskoy group of volcanoes inferred from time-dependent seismic tomography. J Volcanol Geothermal Res (available online). doi:10.1016/j.jvolgeores.2012.10.014

Lees JM (1992) The magma system of Mount St. Helens: non-linear high-resolution P-wave tomography. J Volcanol Geotherm Res 53(1):103–116

Lin FC, Li D, Clayton RW, Hollis D (2013) High-resolution 3D shallow crustal structure in Long Beach, California: application of ambient noise tomography on a dense seismic array. Geophysics 78(4): Q45–Q56. doi:10.1190/geo2012-0453.1

Longuet-Higgins MS (1950) A theory of the origin of microseisms. R Soc Lond Philos Trans Ser A 243:1–35

Masterlark T, Haney M, Dickinson H, Fournier T, Searcy C (2010) Rheologic and structural controls on the deformation of Okmok volcano, Alaska: FEMs, InSAR, and ambient noise tomography. J Geophys Res 115:B02409. doi:10.1029/2009JB006324

DOI 10.1007/978-3-642-36197-5_51-1

Montelli R, Nolet G, Dahlen FA, Masters G, Engdahl ER, Hung SH (2004) Finite-frequency tomography reveals a variety of plumes in the mantle. Science 303(5656):338–343

Nagaoka Y, Nishida K, Aoki Y, Takeo M, Ohminato T (2012) Seismic imaging of magma chamber beneath an active volcano. Earth Planet Sci Lett 333–334:1–8. doi:10.1016/j.epsl.2012.03.034

Paige CC, Saunders MA (1982) LSQR: an algorithm for sparse linear equations and sparse least squares. ACM Trans Math Soft 8:43–71

Patanè D, Barberi G, Cocina O, De Gori P, Chiarabba C (2006) Time-resolved seismic tomography detects magma intrusions at Mount Etna. Science 313(5788):821–823

Paulatto M, Minshull TA, Baptie B, Dean S, Hammond JOS, Henstock T, Voight B (2010) Upper crustal structure of an active volcano from refraction/reflection tomography, Montserrat, Lesser Antilles. Geophys J Int 180(2):685–696

Power JA, Villasenor A, Benz HM (1998) Seismic image of the Mount Spurr magmatic system. Bull Volcanol 60(1):27–37

Ritzwoller MH, Lin FC, Shen W (2011) Ambient noise tomography with a large seismic array. Compte Rendus Geosci. doi:10.1016/j.crte.2011.03.007

Sens-Schönfelder C, Wegler U (2006) Passive image interferometry and seasonal variations of seismic velocities at Merapi Volcano, Indonesia. Geophys Res Lett 33:L21302

Shapiro NM, Campillo M, Stehly L, Ritzwoller M (2005) High resolution surface wave tomography from ambient seismic noise. Science 307:1615–1618

Sharp ADL, Davis PM, Gray F (1980) A low velocity zone beneath Mount Etna and magma storage. Nature 287:587–591

Stankiewicz J, Ryberg T, Haberland C, Fauzi, Natawidjaja D (2010) Lake Toba volcano magma chamber imaged by ambient seismic noise tomography. Geophys Res Lett 37:L17306. doi:10.1029/2010GL044211

Stauber DA, Green SM, Iyer HM (1988) Three-dimensional P velocity structure of the crust below Newberry Volcano, Oregon. J Geophy Res Solid Earth (1978–2012) 93(B9):10095–10107

Thurber CH (1983) Earthquake locations and three-dimensional crustal structure in the Coyote Lake area, central California. J Geophys Res Solid Earth (1978–2012) 88(B10):8226–8236

Thurber CH (1984) Seismic detection of the summit magma complex of Kilauea volcano, Hawaii. Science 223(4632):165–167

Villasenor A, Benz HM, Filippi L, De Luca G, Scarpa R, Patanè G, Vinciguerra S (1998) Three-dimensional P-wave velocity structure of Mt. Etna, Italy. Geophys Res Lett 25(11):1975–1978

Zandomeneghi D, Barclay AH, Almendros J, Ibáñez JM, Wilcock WSD, Ben-Zvi T (2009) Crustal structure of deception island volcano from p-wave seismic tomography: tectonic and volcanic implications. J Geophys Res 114:B06310

Zollo AEA, Gasparini P, Virieux J, Le Meur H, De Natale G, Biella G, Vilardo G (1996) Seismic evidence for a low-velocity zone in the upper crust beneath Mount Vesuvius. Science 274(5287):592–594